

Supplemental information

**miR-107 represses *DMPK* and is sequestered
by CUG repeats triggering the MSI2/miR-7
pathogenesis axis in myotonic dystrophy**

N. Moreno, M. Sabater-Arcis, J. Espinosa-Espinosa, L. Mulet-Rivero, E. García-España, J. González-García, D. Seoane-Miraz, M.J.A. Wood, M.A. Varela, J. Ohana, T. Sevilla, M. Perez Alonso, A. Bargiela, and R. Artero

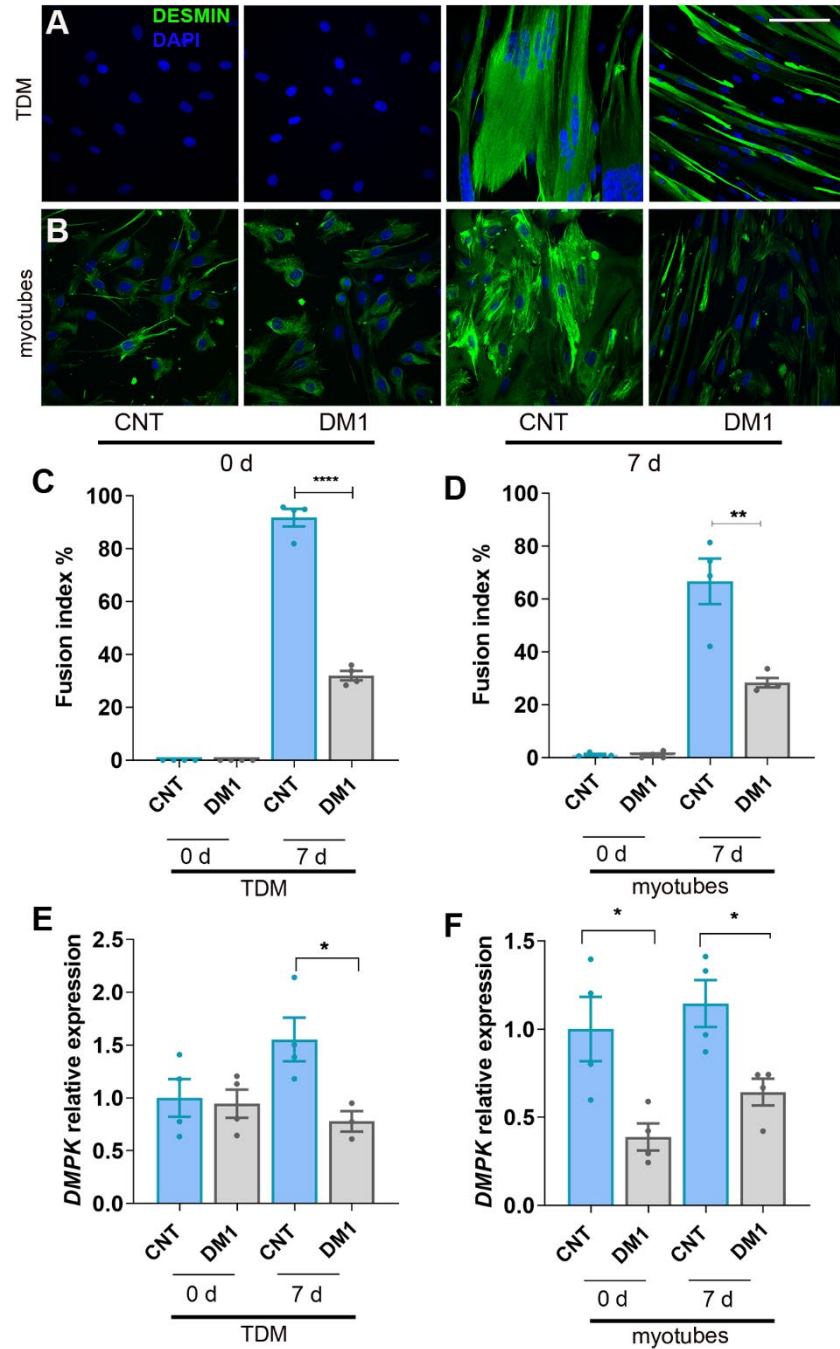


Figure S1. Representative confocal microscopy images of immunofluorescence using an anti-DESMIN antibody (green) in CNT and DM1 TDM **(A)**, or myotubes **(B)** at day 0 and 7 of differentiation. Nuclei were counterstained with DAPI. The scale bar equals 100 μ m. Quantification of fusion index **(C,D)** and *DMPK* relative expression by RT-qPCR **(E,F)** in TDM

(C,E) or myotubes (D,F) at day 0 or 7 of differentiation. *DMPK* transcripts were normalized to the endogenous expression of the mean of *GAPDH*. The bar graphs show mean \pm S.E.M. * $P<0.05$, ** $P<0.01$, **** $P<0.0001$ according to one-way ANOVA test and Tukey's HSD post hoc test when necessary.

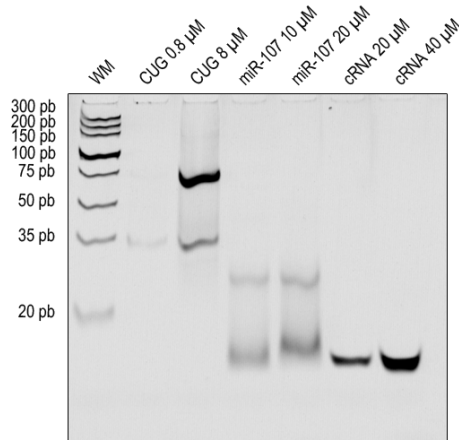


Figure S2. EMSA technical controls for Fig. 2 E-F. Lanes 1 and 2 show the CUG RNA at 0.8 μ M and 8 μ M. Lanes 3 and 4 show miR-107 at 10 μ M and 20 μ M. Lanes 5 and 6 show control RNA (cRNA) at 20 μ M and 40 μ M.

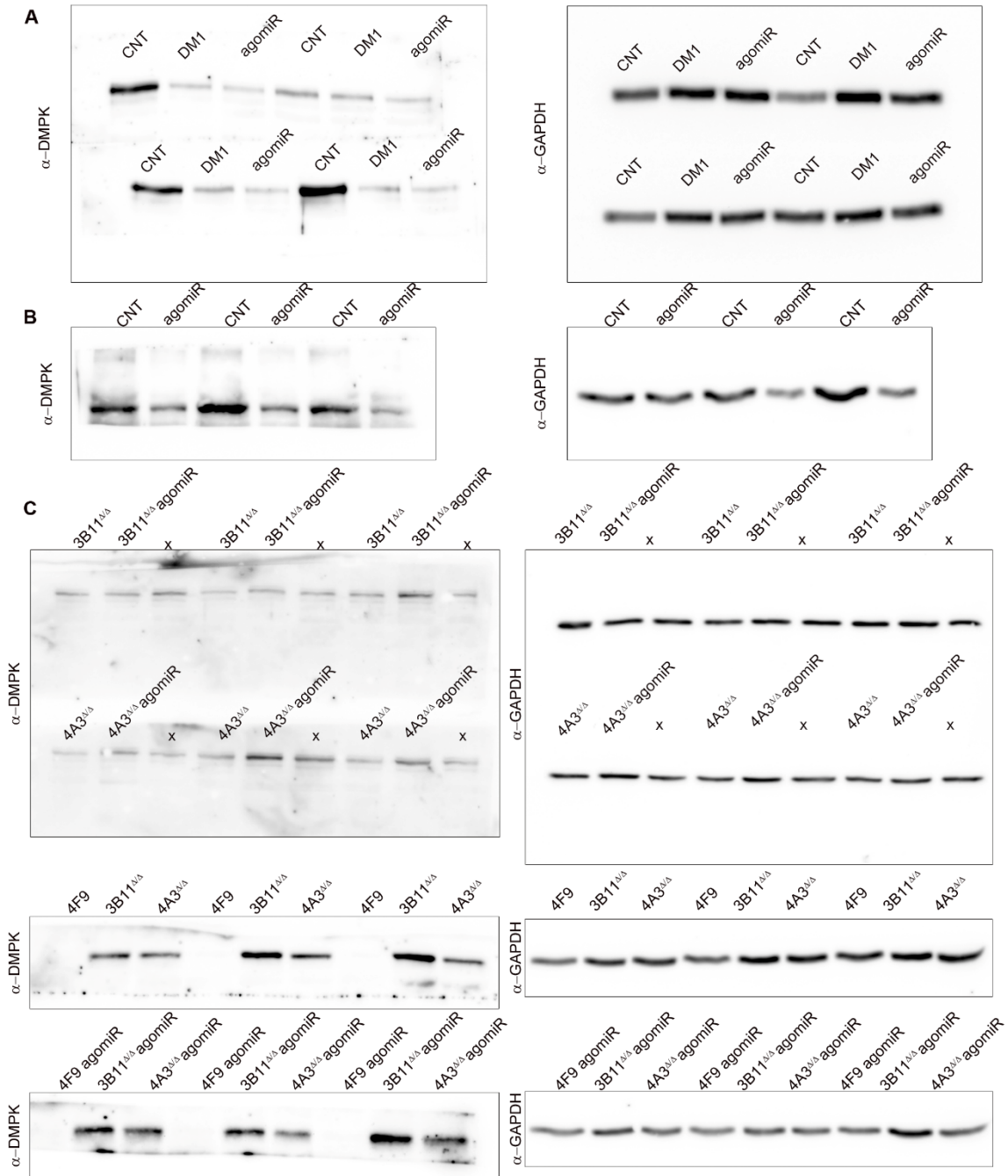


Figure S3. Uncropped western blots for Fig. 3C (A), 3D (B), and Fig. 3F (C). Crosses mark membrane lanes from unrelated experiments. WM: weight marker

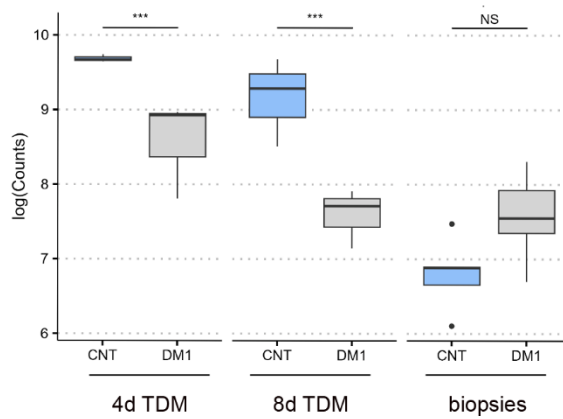


Figure S4. *DMPK* transcripts analyzed from RNAseq data from CNT and DM1 TDM differentiated for 4 and 8 days (n=3) or from biopsies from CNT or DM1 donors (n=5 and 22, respectively). The boxplot represents the normalized *DMPK* expression levels (log-transformed normalized counts). Statistical analysis was performed using the quasi-likelihood F-test implemented in the edgeR package, with statistical significance denoted as NS ($p > 0.05$), ** ($p < 0.01$), and *** ($p < 0.001$). The horizontal line within each box represents the median expression level, while the upper and lower edges of the box correspond to the third and first quartiles, respectively, capturing the interquartile range (IQR). Whiskers extend to the smallest and largest values within 1.5 times the IQR, and any points beyond these are considered outliers.

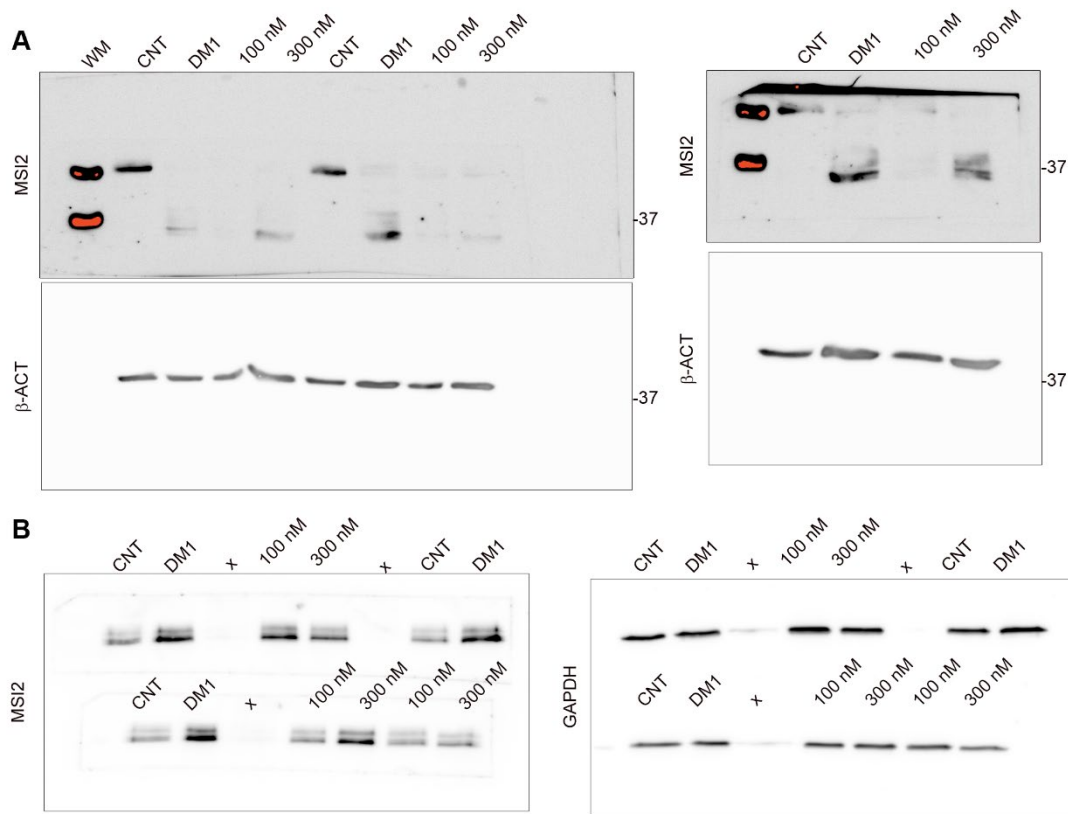


Figure S5. Uncropped western blots for Fig. 5B (A) and Fig. 5C (B). Crosses mark membrane lanes from unrelated experiments. WM: weight marker. Note that as multiple experiments were performed simultaneously with a single control experiment, blot corresponding to β -ACT in panel A is the same as presented in Supplementary Fig. 4B.

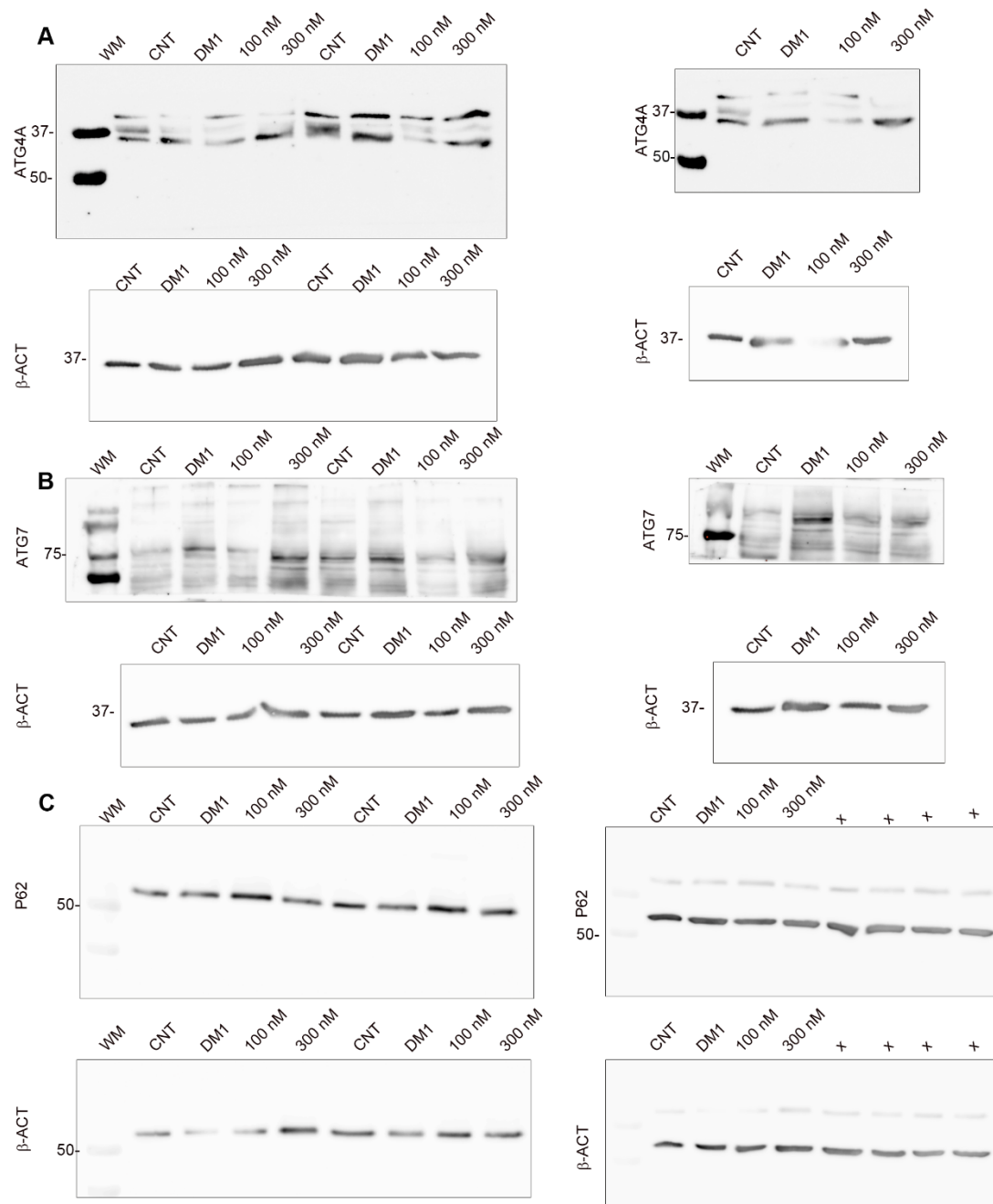


Figure S6. Uncropped western blots for Fig. 6A (A), Fig. 6C (B), and Fig. 6E (C). Crosses mark membrane lanes from unrelated experiments. WM: weight marker

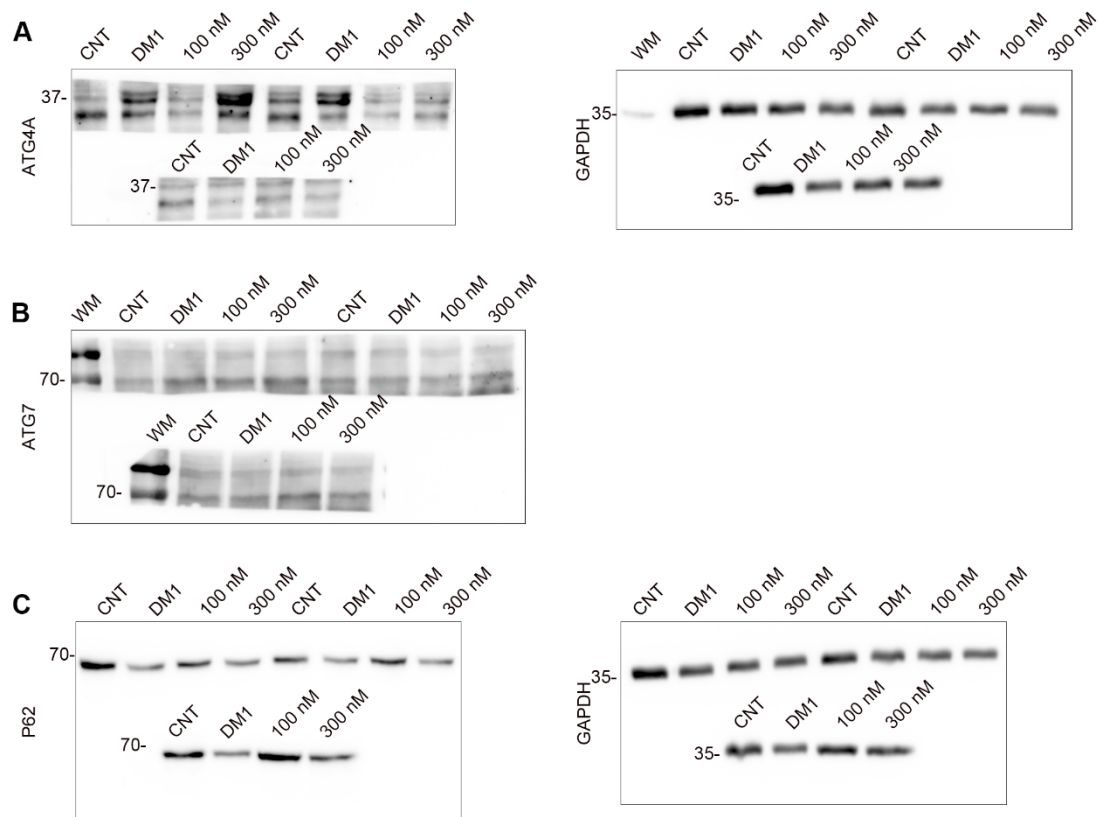


Figure S7. Uncropped western blots for Fig. 6H (A), Fig. 6J (B), and Fig. 6L (C). WM: weight marker. The membrane where GAPDH is immunodetected in panel A also corresponds to that in panel B.

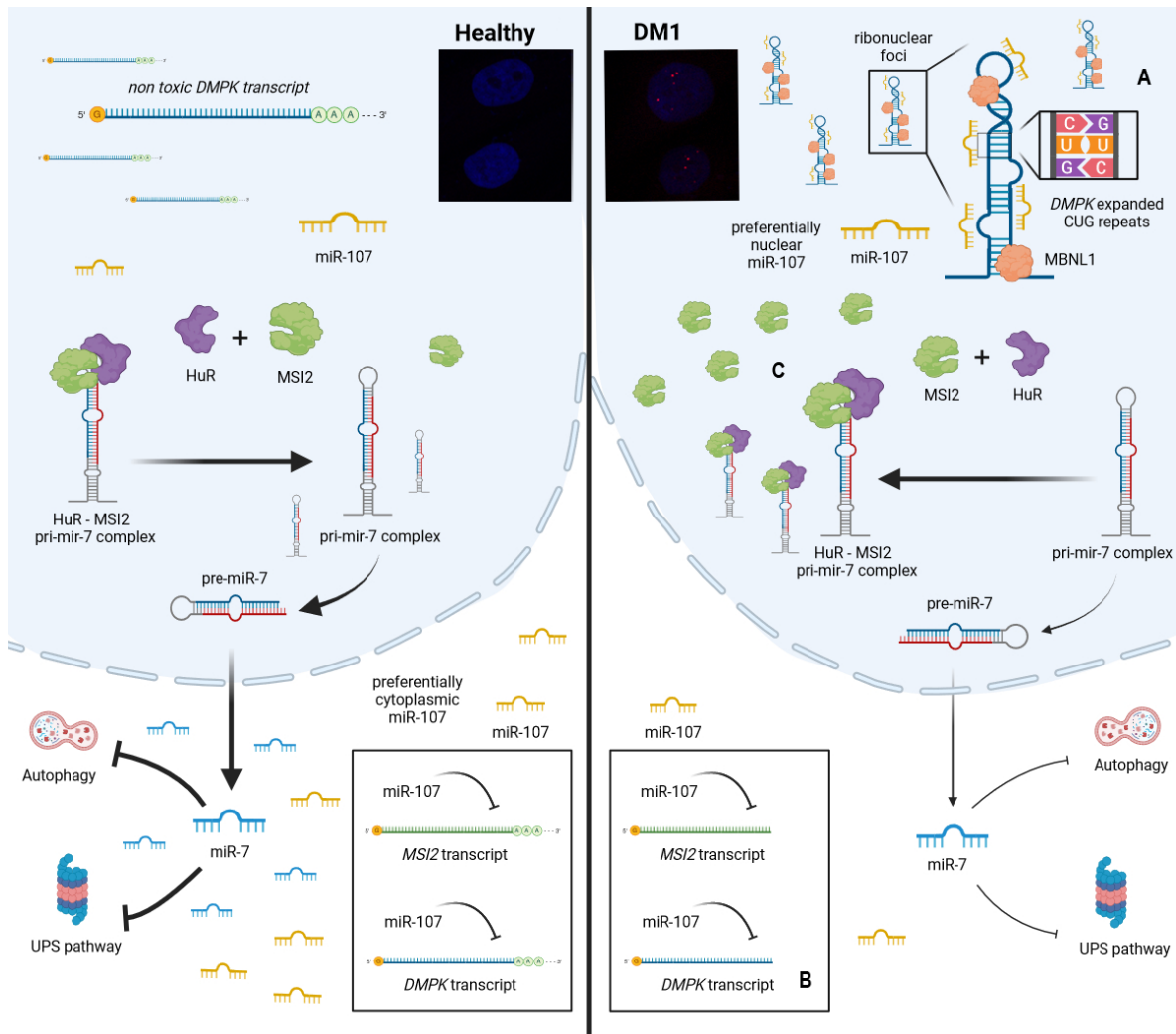


Figure S8. Schematic representation of the model of miR-107 dysregulation and its implications in the MSI2>miR-7>autophagy axis in DM1. (A) In DM1, miR-107 sequestration within ribonuclear foci formed by the expanded CUG repeats in *DMPK* transcript, as with other molecules such as MBNL1, results in the preferential localization of this miRNA within the nucleus, a phenomenon not observed in healthy cells. This disparity in subcellular localization hampers the ability of miR-107 to repress its targets in the cytoplasm, thereby leading to their overexpression, including MSI2. **(B)** *DMPK* is also among the targets of miR-107, and their interaction may stimulate the translocation of mutant *DMPK* transcripts to the cytoplasm, where miR-107 acts as a repressor promoting its degradation. **(C)** The heightened expression of MSI2 in DM1 facilitates the formation of the pri-miR-7-MSI2-HuR

complex, which impedes miR-7 biogenesis by inhibiting the maturation of pre-miR-7. This culminates in diminished miR-7 levels in DM1, which fail to sufficiently repress autophagy and the UPS, thus exacerbating the characteristic imbalance of muscle homeostasis in DM1 by amplifying these catabolic pathways. In contrast, in healthy conditions without ribonuclear foci, miR-107 operates within the cytoplasm to suppress MSI2 expression, ultimately resulting in normal miR-7 levels capable of inhibiting autophagy and the UPS system. Figure created with BioRender.com

Table S1. Genes with a significant up regulation in at least one of the comparisons (biopsies, 4 or 8-days differentiated TDMs) and that were identified as miR-107 target.